

## On the feasibility of monopile foundations for offshore wind in the Baltic Sea

van der Stap, Florian L.; Nielsen, Martin B.; Owen, Cody C.; van der Male, Pim; Hendrikse, Hayo

**Publication date**  
2023

**Document Version**  
Final published version

**Published in**  
Proceedings of the 27th International Conference on Port and Ocean Engineering under Arctic Conditions

### Citation (APA)

van der Stap, F. L., Nielsen, M. B., Owen, C. C., van der Male, P., & Hendrikse, H. (2023). On the feasibility of monopile foundations for offshore wind in the Baltic Sea. In *Proceedings of the 27th International Conference on Port and Ocean Engineering under Arctic Conditions* (Proceedings - International Conference on Port and Ocean Engineering under Arctic Conditions). POAC.

### Important note

To cite this publication, please use the final published version (if applicable).  
Please check the document version above.

### Copyright

Other than for strictly personal use, it is not permitted to download, forward or distribute the text or part of it, without the consent of the author(s) and/or copyright holder(s), unless the work is under an open content license such as Creative Commons.

### Takedown policy

Please contact us and provide details if you believe this document breaches copyrights.  
We will remove access to the work immediately and investigate your claim.



## **On the feasibility of monopile foundations for offshore wind in the Baltic Sea**

Florian L. van der Stap<sup>1</sup>, Martin B. Nielsen<sup>1</sup>, Cody C. Owen<sup>2</sup>, Pim van der Male<sup>2</sup>, Hayo Hendrikse<sup>2</sup>

<sup>1</sup> Wood Thilsted Partners, Tolbodgade 51B, DK-1253 Copenhagen, Denmark

<sup>2</sup> Delft University of Technology, Department of Hydraulic Engineering, Delft, The Netherlands

### **ABSTRACT**

For the design of offshore foundations in regions such as the Baltic Sea, it is paramount that ice-structure interaction is appropriately considered. For the monopile, a common foundation for offshore wind turbines, challenges with ice-induced vibrations and high ridge loads may require ice-mitigating measures to be included in the design. A ‘feasibility map’ showing the necessity for such ice-mitigating measures in the entire Baltic region has been developed for monopiles. The feasibility was considered in technical terms by imposing design, installation, and fabrication constraints, and in economic terms, expressed in weight increase of monopiles when compared to an ‘ice-free’ design. A design assessment of offshore wind turbines across the Baltic Sea was conducted by optimizing foundation designs for the IEA 15 MW reference turbine for nine identified characteristic regions of the Baltic Sea. The assessment was performed via the in-house foundation design software MORPHEUS by Wood Thilsted. MORPHEUS has been coupled to the phenomenological ice model “VANILLA” to capture the dynamic ice-structure interaction for level ice. From the assessment, the following regions are deemed feasible for monopiles without ice-mitigating measures: the Danish Straits, the Baltic Proper South, the Baltic Proper North, the Gulf of Riga and the Archipelago Sea. The Bothnian Sea North and the Bay of Bothnia are deemed infeasible without mitigating measures. For the Bothnian Sea South and the Gulf of Finland, no conclusive answer was found as more research into the cost competitiveness of alternative options is required. The increase in fatigue resulting from ice loading was found to be the main cause for foundation weight increase of monopiles compared to monopiles designed for ice-free waters.

**KEY WORDS:** Ice crushing; monopile design; ice-induced vibrations; ridge loads.

### **INTRODUCTION**

Offshore wind has seen a steep increase in popularity in the past decade due to the worldwide commitment to combat climate change. As a result, the offshore wind industry is starting to explore regions traditionally considered to have severe environmental conditions, such as the presence of sea ice. The Baltic Sea is such a region, as various subregions are known to be ice-infested on a yearly basis (Jevrejeva et al., 2004). The Baltic Sea also has been reported to have significant potential for growth, with reports of a potential capacity of up to 93 GW (European Commission and Directorate-General for Energy, 2019).

The monopile is likely to be the preferred foundation for the development of offshore wind in the Baltic Sea. The foundation type is relatively mature and usually yields the lowest Levelized Cost of Energy (LCOE) due to its simple nature in both design and installation (Wu et al., 2019; WindEurope, 2020). The presence of ice has been estimated to not adversely affect the foundation design in the Southern Baltic Sea, due to the relatively low magnitude of ice loads and low occurrence frequency of sea ice in this region (Gravesen and Kärnä, 2009). However, given the severity of ice seasons in the northern and eastern regions of the Baltic Sea (Jevrejeva et al., 2004), and the corresponding potential development of severe ice-induced vibrations, mitigating measures might be necessary once wind farm development expands into these areas.

Typical ice mitigating measures include the installation of ice cones at the ice action point or the use of a sloping Gravity Based Structure (GBS) over a monopile. The slope of an ice cone or a GBS alters the ice failure mode from crushing to bending, greatly reducing the global load. However, ice cones negatively affect the LCOE due to expensive fabrication and post-installation costs. Post-installation of cones is typically required since driving foundations with cones is not feasible. Additionally, the reduced accessibility caused by the presence of cones makes maintenance activities more challenging. Furthermore, the foundation is subject to significantly higher wave loading due to the increased diameter at the waterline (Tang et al., 2021; Zhu et al., 2021). A GBS is typically limited to shallow waters, as it becomes less cost-effective for greater water depths (Wu et al., 2019).

Implementation of mitigation measures significantly increases the cost estimates for competitive bids. Hence, the utilization of early-phase screening tools to evaluate the need for mitigating measures is extremely beneficial. For the present study, the goal was to define a ‘feasibility map’ for monopile foundations in the Baltic Sea. Such a map can be of value in early project phases when foundation concepts are to be decided upon, as well as for defining relevant research avenues as it reveals the most relevant ice design load cases (DLCs) and associated uncertainties.

The present study is structured as follows. First, characteristic regions in the Baltic Sea are defined based on relevant metocean data. This is followed by the introduction of the approach to assessing feasibility of monopile foundations for offshore wind turbines. Finally, the resulting feasibility map is presented and discussed, indicating the most relevant ice-structure interaction scenarios and uncertainties therein.

## **DEFINITION OF CHARACTERISTIC REGIONS IN THE BALTIC SEA**

To define a high-level feasibility map for the Baltic Sea, it is necessary to identify and classify distinct regions, each with their own representative metocean data. In addition to conventional wind, metocean, and bathymetry data, ice conditions are crucial for evaluating the feasibility of monopile structures in the Baltic Sea. As the main focus of the present study was on ice loading, priority was given to parameters that have a significant impact on ice loading, such as level ice properties, ice ridge properties, the ice crushing coefficient ( $C_R$ ), and the number of ice interaction days in each region. This section describes the process of determining these parameters and the resulting characteristic regions used in the study.

The ice thickness was evaluated using air temperature datasets from various weather stations in Estonia, Finland, Germany, Latvia, Poland, and Sweden (respective weather institutes: DW, FMI, IMGW, ILM, LVGMC, and SMHI). Prior research has shown that air temperature data

can provide reasonable estimates of the ice thickness (Stefan, 1891; Leppäranta, 1993). The ice thickness was determined with the following relation, derived from ISO 19906 (2019):

$$h_{ice} = \sqrt{\omega \frac{2k_{ice}}{\rho_{ice}l} C_{FDD}} \quad (1)$$

where  $\omega$  is an empirically derived coefficient typically between 0.3-0.7 according to ISO 19906 (2019),  $k_{ice}$  is the thermal conductivity of ice,  $\rho$  is the ice density,  $l$  is the latent heat of fusion of water and  $C_{FDD}$  is the number of cumulative freezing degree days. Equation (1) was used to obtain the ice thickness for each year and each location where temperature measurements were available with an  $\omega$  of 0.55. A Generalized Extreme Value fit was applied to the yearly data to determine the 50-year extreme ice thickness, which was interpolated over the entire Baltic Sea region to create a map. The 50-year extreme ice thickness was selected as it serves as a measure of ice condition severity and it is required for Ultimate Limit State (ULS) analysis, as specified in the design standards (DNV-GL, 2016; IEC, 2019). The data were further scaled and validated against existing ice thickness measurements and ice charts (van der Stap, 2022). The resulting ice thickness map, including a boundary between landfast and drift ice, is shown in Figure 1 (left). It is noted that this map does not account for, for example, the possibility of former landfast ice drifting into warm regions at the end of the season.

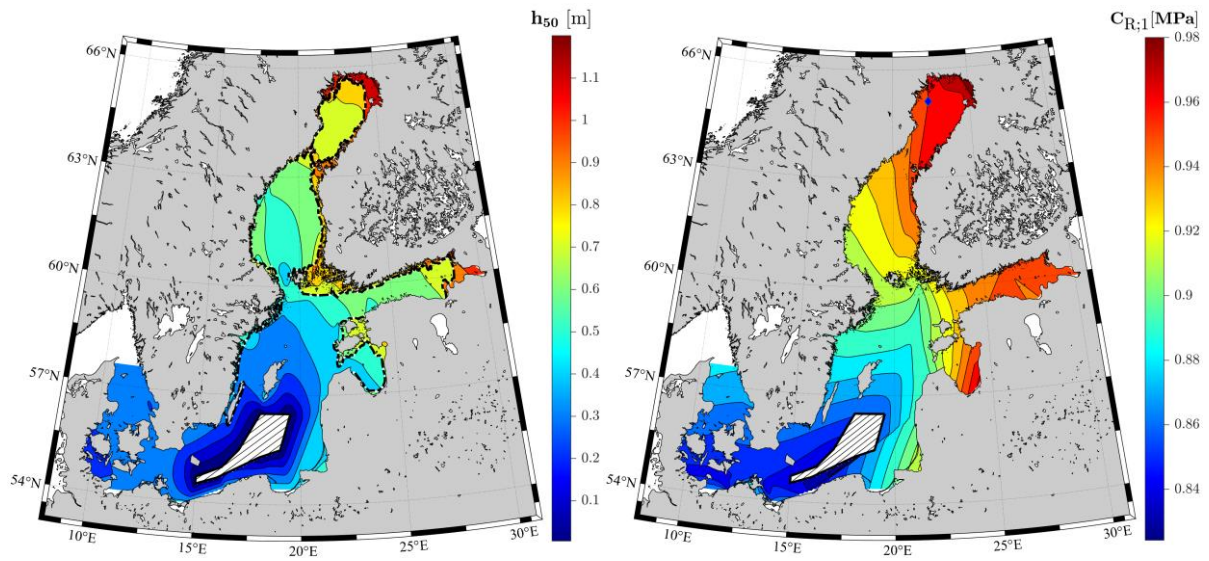


Figure 1. Design ice thickness (left),  $h_{50}$ , for a 1/50-year ice event and ice strength coefficient (right),  $C_{R;1}$ , for a 1/1-year ice event in the Baltic Sea. The hatched area defines the area where no ice is predicted based on the method used ( $< 0.05$  m ice thickness), even in extreme winters. The dash-dotted line indicates the boundary between landfast and drift ice (van der Stap, 2022).

Secondly, the ice ridge loads per region were assessed. Level ice often deforms into ice ridges due to the wind and currents forcing ice-ice interaction. This is particularly prevalent at the boundaries between landfast and drift ice as the mobile drift ice is pushed into the stationary landfast ice. The presence of a windfarm may have a similar effect as landfast ice; therefore, an accurate assessment of ice ridges is crucial for design. Currently, there is no data available on ice ridge formation in the Southern Baltic Sea, as it is a relatively infrequent phenomenon. The calculation of the ridge action usually ignores the sail of the ridge. The total ridge action

was then calculated as the sum of the action due to the consolidated layer and the keel (ISO 19906, 2019). To determine the consolidated layer thickness, guidelines from the IceStruct JIP (DNV, 2013), were applied, namely  $h_c = 1.5 \cdot h_{50}$ . The consolidated layer action was calculated with the ice crushing formula from ISO 19906 (2019).

Two differing ridge keel action were considered based on two sets of parameters, with only the keel cohesion,  $c$ , varying between the two. This approach was adopted as the proposed value for  $c$  in the ISO 19906 was potentially conservative, and previous research indicate in the Bay of Bothnia indicate alternative values (Heinonen, 2004).

The parameters used to determine ridge actions in the present study are summarized in Table 1. The alternative value for the keel cohesion is based on a relation between the cohesion and the internal friction angle of ice ridges in the Bothnian Bay (Heinonen, 2004). The highest value found in the research (6.5 kPa) is applied at the Bay of Bothnia, while the lowest value (3 kPa) is assumed in the southern regions. Note, there is no research on the variation in magnitude of the keel cohesion between mild and severe ice regions. It is an assumption that with lesser freezing degree days the cohesion would be lower. The keel cohesion in the other regions was scaled based on the length of the ice season. Finally, the keel action was calculated using the relevant equations from ISO 19906 (2019).

Table 1. Ice ridge parameters according to design standards (ISO 19906, 2019; Det Norske Veritas AS, 2013) and field research.

Ridge parameter	Description	Design standards	Alternative
$h_c$	Consolidated layer thickness	$1.5h_{50}$	$1.5h_{50}$
$h_k$	Keel height	$12.5\sqrt{h_{50}}$	$12.5\sqrt{h_{50}}$
$e$	Porosity	0.3	0.3
$\varphi$	Internal friction angle	$35^\circ$	$35^\circ$
$c$	Keel cohesion	10 kPa	3-6.5 kPa

ISO 19906 suggests various methods to derive a representative ice strength coefficient  $C_R$ . The most common method for the Baltic Sea, a temperate region, is to apply the  $C_R$  obtained from measurements in the Bay of Bothnia—a region known for its severe ice conditions—to the entire Baltic Sea (ISO 19906, 2019). However, the original derivation of the  $C_R$  coefficient included the effects of ice exposure and the average temperature of the ice, which is highly variable throughout the Baltic Sea, as is the salinity which is also known to affect the crushing strength of ice (Kärnä & Qu, 2006; Timco & Frederking, 1983). As a result, applying the  $C_R$  value derived from Bay of Bothnia experiments to the entire Baltic Sea would lead to overly conservative ice load estimates.

Consequently, a novel method for  $C_R$  scaling was introduced. This method takes into account the length of the ice season, which is assumed to be an appropriate indicator of exposure. A large-scale statistical analysis of ice seasons was used as this included long-term data for the entire region (Jevrejeva et al., 2004). By assuming similar drift conditions throughout the Baltic Sea, the annual maximum value of  $C_R$  at the reference location, the Norströmsgrund Lighthouse, was correlated to the  $x$ -year maximum at various locations in the Baltic Sea based on the length of the ice season. For example, the annual maximum value of  $C_R$  at the lighthouse (with an ice

season of 168 days) corresponds to a 6.2-year maximum for Ustka, Germany, assuming an ice season duration of 27 days. Subsequently, a reduction factor to scale the  $C_R$  at the Noströmsgrund Lighthouse is found by relating the return period to the extreme global pressure as determined in experiments at the Lighthouse (Gravesen & Kärnä, 2009). The resulting  $C_R$  coefficients for all observation stations were interpolated over the Baltic Sea as presented in Figure 1 (right). In region with more severe ice drift than in the Bay of Bothnia this approach may be unconservative as this would yield more exposure of structures to ice and a higher  $C_R$  value.

For the evaluation of the Fatigue Limit State (FLS) in the design load cases, the probability of each ice state and the number of ice interaction days during the lifetime of the structure were assessed. The ice velocity was found to be 2% of the wind velocity, since previous research has shown that, in the Baltic Sea, a wind factor model is comparable to fully coupled ice-ocean models (Leppäranta and Omstedt, 1990). This factor ignores the presence of wind farms, which may significantly affect the ice drift. Ice thickness distributions were estimated for each region based on research in the Danish Straits and the Bay of Bothnia (Hornnes et al., 2022; Hornnes et al, 2020; Ronkainen et al. 2018). The number of ice interaction days,  $D_{ice}$ , was estimated based on the probability of ice occurrence at the coast, a correction for ice formation offshore, and an ice drift factor based on experiments at the Noströmsgrund Lighthouse. The values were consistent with those found in previous studies (Thijssen et al., 2019; Hornnes et al., 2022).

Besides the ice conditions, representative values were found for wind, waves, bathymetry, and currents. Based on the divisions of the Baltic Sea into characteristic regions for wind and wave conditions, and the results in Figure 1, the following nine characteristic regions were defined: the Danish Straits, the Baltic Proper South, the Baltic Proper North, the Gulf of Riga, the Gulf of Finland, the Archipelago Sea, the Bothnian Sea South, the Bothnian Sea North and the Bay of Bothnia (see Figure 2).

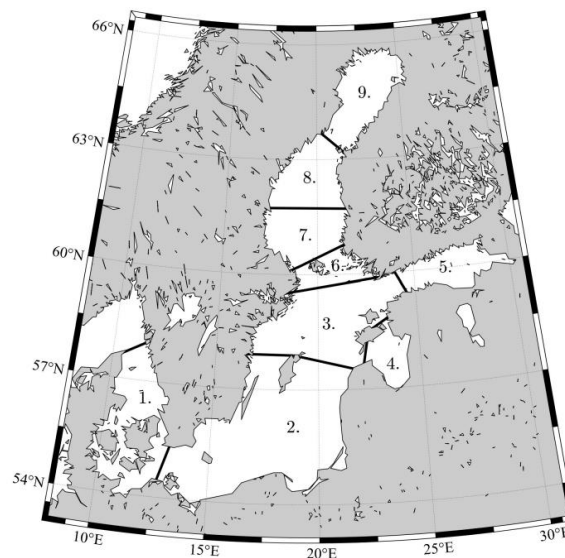


Figure 2. The nine identified characteristic regions of the Baltic Sea. 1 - the Danish Straits, 2 - the Baltic Proper South, 3 - the Baltic Proper North, 4 - the Gulf of Riga, 5 - the Gulf of Finland, 6 - the Archipelago Sea, 7 - the Bothnian Sea South, 8 - the Bothnian Sea North, and 9 - the Bay of Bothnia.

Table 2 presents representative ice parameters, 50-year extreme wind,  $v_{\text{wind};50}$ , and 50-year extreme wave height,  $H_{S;50}$ , for each region. Representative wind and wave tables, extreme sea states, and bathymetry profiles were compiled for each individual region, while the soil profiles, ice drift speeds, and current velocities were kept constant for each region. To access the specific values used in the present study, reference is made to van der Stap (2022), which provides more detailed information per region.

Table 2. The nine identified regions in the Baltic Sea and a sample of their characteristic ice, wind, and wave conditions (van der Stap, 2022).

Region no.	Region	$h_{50}$ [m]	$C_{R;1}$ [MPa]	$v_{\text{wind};50}$ [m/s]	$H_{S;50}$	$D_{\text{ice}}$ [days/lifetime]
1	Danish Straits	0.40	0.88	45.06	6.17	9.6
2	Baltic Proper S.	0.45	0.86	43.44	12.43	11.9
3	Baltic Proper N.	0.50	0.88	43.88	12.96	73.3
4	Gulf of Riga	0.55	0.94	39.19	9.23	197.6
5	Gulf of Finland	0.95	0.95	35.96	6.44	198.0
6	Archipelago Sea	0.75	0.92	40.28	6.55	96.9
7	Bothnian Sea S.	0.65	0.92	40.72	12.53	228.0
8	Bothnian Sea N.	1.00	0.92	41.07	11.26	299.8
9	Bay of Bothnia	1.25	0.98	37.70	9.75	352.5

## FEASIBILITY ASSESSMENT

The feasibility for monopiles was investigated by conducting a design procedure for the IEA 15 MW reference turbine for each identified region in both a ‘non-ice’—or reference case—and an ‘ice’ case (see Figure 4). For the reference case, the following DLCs were selected according to DNV-GL (2016): DLC1.4, 1.6, and 6.1 for the ULS and DLC1.2, 6.4, and 7.2 for FLS. The design procedure for the ice case included the five load cases as prescribed by DNV-GL (2016) and listed in Table 3.

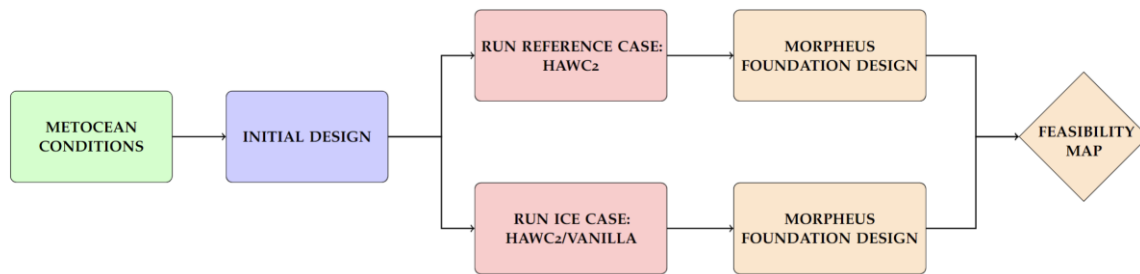


Figure 4. Research method for the development of a monopile feasibility map in the Baltic Sea. The procedure is executed for each identified region.

The nine regions were each divided into three clusters—shallow, intermediate, and deep—with varying water depth based on their bathymetry. For each design cluster, an initial geometry was



designed in the foundation design framework by Wood Thilsted for offshore wind turbines called MORPHEUS. This framework included a fully automated, highly efficient algorithm for the efficient design of monopiles, in which—for a given pile diameter  $D$ —the embedded pile length  $L_{\text{pile}}$  and wall thickness  $t$  are optimized (Nielsen et al., 2022).

Table 3. DNV-GL and IEC listed ice DLCs (DNV-GL, 2016; IEC, 2019). The fourth column indicates the relevant wind speeds at hub height,  $v_{\text{hub}}$ , for each DLC. The following notation is used for wind speed: cut-in,  $v_{\text{in}}$ , cut-out,  $v_{\text{out}}$ , rate,  $v_{\text{rated}}$ , and  $v_{50}$ , 50-year extreme. For FLS the velocity of the ice sheet was modelled as 2% of the wind speed 10 m above the water level,  $v_{10}$ , and for ULS the ice speed varied between 0.01 and 0.2 with a discretization of 0.01 for the lowest velocities, and 0.02 for velocities above 0.04.

DNV-GL	IEC	Limit state	$v_{\text{hub}}$ [m/s]	$v_{\text{ice}}$ [m/s]
DLC 9.1	DLC D3	ULS	$v_{\text{in}} < v_{\text{hub}} < v_{\text{out}}$	0.01:0.01:0.04 0.06:0.02:0.2
DLC 9.2	DLC D4	FLS/ULS	$v_{\text{in}} < v_{\text{hub}} < v_{\text{out}}$	$0.02v_{10}$
DLC 9.3	DLC D6	ULS	$v_{\text{rated}}, v_{\text{out}}, v_{50}$	0.01:0.01:0.04 0.06:0.02:0.2
DLC 9.4	DLC D7	FLS/ULS	$v_{\text{hub}} < v_{\text{in}}$ $v_{\text{out}} < v_{\text{hub}} < 0.7v_{50}$	$0.02v_{10}$
DLC 9.5	DLC D8	ULS	$v_{50}$	0.01:0.01:0.04 0.06:0.02:0.2

Coupled aero-elastic ice-structure interaction simulations were run in the novel software integration of the HAWC2 aero-elastic model (Rinker et al., 2020), and the ice-structure interaction model, VANILLA (Hendrikse & Nord, 2019). With MORPHEUS, optimized designs were generated for the ‘non-ice’ and the ‘ice’ cases based on loads derived from the relevant simulations.

In the final iteration, design, fabrication, and installation constraints were imposed to demark the ‘feasibility’ of each design. The design constraints were set to satisfy ULS and FLS capacity checks, as well as specified dynamic properties of the foundation. The fabrication constraints included a maximum  $D/t$  ratio of 130 and 180 for the monopile and the transition piece, respectively, a maximum wall thickness of 150 mm, a maximum can weight of 100 tonnes, and a can height range of 2000-4200 and 2000-3500 mm for cylindrical and conical cones, respectively. The fabrication constraint limited the maximum weight of the monopile to 2000 tonnes. The designs were then compared and verified against these constraints to create a feasibility map.

## RESULTS

Figure 5 shows the calculated ULS overturning moment load envelopes in the mildest and the most severe ice regions, the Danish Straits and the Bay of Bothnia, respectively. The load envelopes for all other regions indicated that as ice conditions worsened, the load envelope was increasingly more governed by the ice DLCs, which was in line with expectations. Similar results were found for the fatigue DLCs, in which the damage equivalent moment increased for increasing ice thickness and ice interaction days.



During load generation, only the 50-year extreme ice thickness combined with a 1-year nominal  $C_R$  were simulated and no other combinations were considered. For the time domain simulations, it was also assumed that the limit stress was governing over the limit force and limit energy; i.e. driving forces were always sufficient for ice failure and constant ice drift. However, with increasing size of the foundations this may be unrealistic as ice sheets—especially ridges—could come to halt against the structures (Croasdale, 1984).

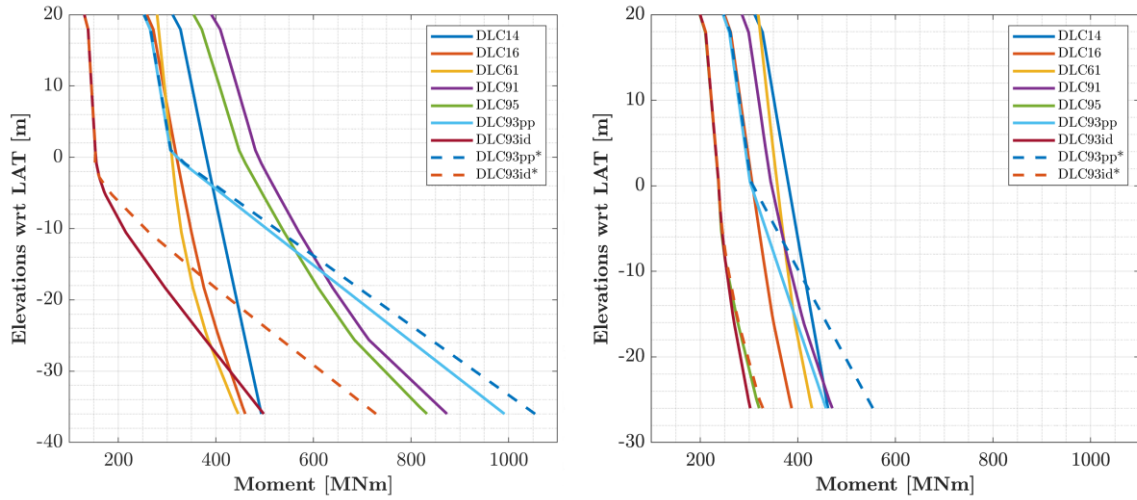


Figure 5. Extreme overturning moment load envelopes in (left) the Bay of Bothnia and (right) the Danish Straits. For DLC 9.3 (the ice ridge) both the idling (id) and power production (pp) are considered, the latter of which is not required by IEC61400-3-1 (2019). The ridge action using a keel cohesion of 10 kPa (see Table 1) is indicated by the dashed lines.

The resulting load effect is illustrated in Figure 6, which indicates the change in foundation mass,  $\Delta M_F$ , between the ‘reference’ and ‘ice’ case, if all the design and fabrication constraints were satisfied. It should be noted that water depth was region specific as outlined in Table 4.

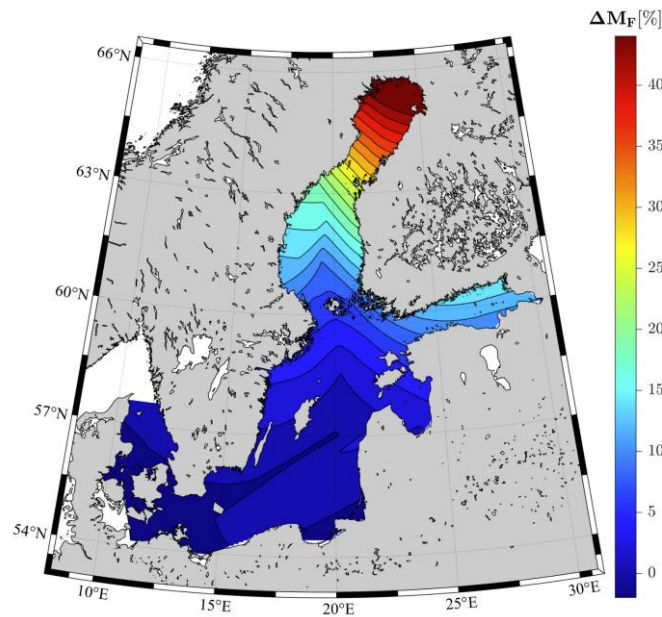


Figure 6. Change in foundation mass,  $\Delta M_F$ , when a monopile design for ice is compared to an ice-free design in the Baltic Sea for the simulated water depth in each region (25–45 m).

Based on the resulting designs, weight increases, and utilizations ratios, monopiles in the Danish Straits, Baltic Proper South, Baltic Proper North, Gulf of Riga, and Archipelago Sea were deemed feasible (see Figure 7). In the cases of the Baltic Proper North, the Gulf of Finland, and the Bothnian Sea South, the overall structural stiffness had to be increased to reduce fatigue loads. Without increased stiffness and reduced fatigue damage, the fabrication constraints were not satisfied as the maximum can weights were exceeded. Here, a flexibility parameter  $\alpha_k$ , defined as the lateral deflection at mean sea level under 1 MN static point load, was used as a measure for stiffness. For the Bothnian Sea North and the Bay of Bothnia, fabrication constraints for can weight and can thickness were consistently exceeded until the stiffness was increased by 23% and 42%, respectively. The results are summarized in Table 4.

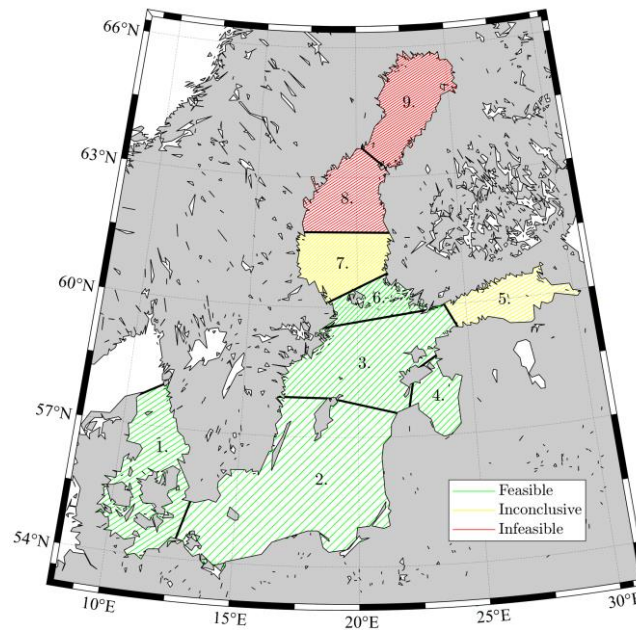


Figure 7. Feasibility map for monopiles without ice-mitigating measures in the Baltic Sea for region-specific water depths.

Table 4. Summary of results for monopile design optimization in terms of monopile weight,  $M_{MP}$ , and monopile flexibility,  $\alpha_k$ .

Region no.	Region	Depth [m]	Reference case		Ice case	
			$M_{MP}$ [t]	$\alpha_k$ [mm MN <sup>-1</sup> ]	$M_{MP}$ [t]	$\alpha_k$ [mm MN <sup>-1</sup> ]
1	Danish Straits	25	910	9.9	907	9.9
2	Baltic Proper S.	45	1911	14.8	1907	14.9
3	Baltic Proper N.	45	1913	14.9	1964	14.3
4	Gulf of Riga	25	912	9.9	937	9.9
5	Gulf of Finland	35	1306	12.8	1447	12.3
6	Archipelago Sea	25	915	9.9	977	9.7
7	Bothnian Sea S.	35	1341	12.4	1464	11.9
8	Bothnian Sea N.	45	1821	15.9	2178	12.9
9	Bay of Bothnia	35	1323	12.8	1930	8.9

As a result of the observed weights and utilizations, monopile designs without ice-mitigating measures were deemed infeasible in the Bothnian Sea North Bay and the Bay of Bothnia. By adhering to fabrication constraints, inefficient and unrealistic designs were required, and in the case of the monopiles in the Bothnian Sea North, installation constraints were also exceeded.

Monopile feasibility for the Bothnian Sea South and the Gulf of Finland region was difficult to assess and likely requires further research. An efficient design that satisfied all criteria was possible. However, a substantial weight increase was observed (10–13%), which, despite the technical feasibility, may indicate economic infeasibility. For the Gulf of Finland, it should be noted that the mild wave conditions play a role. As a result, the wave contribution to the total fatigue damage was low compared to other regions. However, the increased weight was still substantial and should be compared to alternative solutions with ice-mitigating measures. Figure 7 presents the final feasibility map, for region-specific water depths, for monopiles without ice-mitigating measures in the Baltic Sea.

## DISCUSSION

A strong correlation was found between the feasibility of the monopiles and the lifetime fatigue damage. Although ULS load envelopes were shown to be governing, additional pile length would be sufficient to deal with the ULS loads. From the design framework MORPHEUS, it was found that at elevations of the foundation, which showed exceedance of design and fabrication constraints, the designs were often driven by fatigue loads. The method for ridge calculation (see Table 1) had a negligible effect on the weight per monopile, which again indicates that the weight increase was primarily driven by increased fatigue from ice in the regions with more severe ice conditions.

Considering the fatigue damage due to ice loading, ice-structure interaction with level ice at low drift speeds resulting in ice-induced vibrations was the major contributor, with damage of over 90% from ice-induced fatigue damage. This was further confirmed by a sensitivity analysis for the number of ice interaction days, which indicated that by reducing the number of interaction days by 50%, the resulting weight decrease was (especially for the severe regions) close to 50%. It should be noted that, in general, there are few data available about the ice conditions of the Baltic Sea outside a few subregions. As the fatigue is shown to be highly influential, the necessity for research into the frequency of ice occurrence, the ice velocity distribution, and the ice thickness distribution is further emphasized here. Additionally, the research assumed that limit stress was governing, whereas the required driving forces may not always be present, thus reducing the duration of ice-interaction.

Given that the fatigue damage from dynamic ice-structure interaction is so important, it is also relevant to reflect on the choice of the ice strength coefficient. The approach used here defined a region-specific ice strength coefficient which was then used to obtain an estimate for the peak brittle crushing load in simulations. The ice model (Hendrikse and Nord, 2019) then accounted for the velocity and compliance effects, resulting in a load exceeding the ISO 19906 crushing load for the specific ice strength coefficient when intermittent crushing developed. This is a somewhat conservative approach, as for example in the Bay of Bothnia, the effective value for  $C_R$  during intermittent crushing was about 1.91 MPa. This exceeded the regional value of 1.8 MPa as suggested in ISO 19906 to be used to determine the maximum loads during intermittent crushing. A more detailed discussion on this topic can be found in Hendrikse & Owen (2023, this conference). When the ice strength coefficient used for design can be reduced compared

to the values used in this study, the Bothnian Sea South and the Gulf of Finland may become feasible regions.

A preliminary investigation into the effect of water depth was performed by simulating an additional deeper water depth, 45 m, for the Bothnian Sea South region. The results showed that although the effect of ice loading was similar to the effect at intermediate water depth, the resulting weight increase exceeded certain constraints. In this case, the installation constraint of total weight was exceeded. Based on these results, Table 5 presents a preliminary indication of feasibility per region per water depth.

Table 5. Increased weight in percentages for a monopile within a specific region, comparing ice against ice-free design, as well as feasibility of monopiles (green - feasible, orange - inconclusive, red – infeasible, gray - unknown) in the Baltic Sea.

Region	Danish Straits	Baltic Proper S.	Baltic Proper N.	Gulf of Riga	Gulf of Finland	Archipelago Sea	Bothnian Sea S.	Bothnian Sea N.	Bay of Bothnia
Shallow (25 m)	0			3		8			
Intermediate (35 m)					13		10		42
Deep (45 m)		0	2				9	17	

It seemed that monopiles in the Gulf of Riga were possible for intermediate water depths, as conditions were less severe than those in the Gulf of Finland, which was shown to be close to feasible. Inversely, monopiles in the Bothnian Sea North were infeasible for intermediate depth as the Bothnian Sea North had more severe conditions than the South region.

Finally, a recent study by the European Commission has indicated that the potential capacity for offshore wind in the Baltic Sea is estimated at 93.5 GW (European Commission and Directorate-General for Energy, 2019). A comparison between the locations of potential capacity reported in that study and feasible regions in the present study shows that 58.5 GW or 63% (Denmark, Germany, Poland, Lithuania, and Latvia) lies within the green region and another 20 GW or 21% lies partly in green regions (Swedish coastline). While this is a generalization which neglects that the current study focused on a single water depth per region, it nevertheless indicates that large offshore wind farms are likely possible using the preferred monopile foundation without a need for ice-mitigating measures.

## CONCLUSION

The findings of the present study indicated that, from both a technical and economic perspective, monopile designs without ice-mitigating measures were feasible in the Danish Straits, the Baltic Proper South, the Baltic Proper North, the Gulf of Riga and the Archipelago Sea. The design of monopiles for the Bothnian Sea North and the Bay of Bothnia without ice-load-mitigating measures resulted in excessive weight and inefficient designs. The analysis revealed that fatigue damage resulting from ice-induced vibrations, originating from the dynamic interaction with level ice, has a significant impact on the design. The need for substantial increases in stiffness due to the extreme ice thickness and frequency of ice interactions resulted in designs that were deemed infeasible, either technically or economically. Furthermore, while monopile designs in the Bothnian Sea South and the Gulf of Finland were technically feasible without ice-mitigating measures, alternative design options should be

thoroughly investigated, as the increased weight raises concerns about economic feasibility. It is further noted that when uncertainty with respect to the ice strength coefficient used for design for intermittent crushing is reduced, these regions may become feasible as well.

## REFERENCES

Croasdale, K. (1984). The limiting driving force approach to ice loads. *In Offshore Technology Conference*. OnePetro.

Det Norske Veritas AS (2013). Icestruct jip guideline: Ice actions and actions effects on offshore structures. *Geneva: ISO*.

Deutscher Wetterdienst - DW (n.d.). Observation data - Open Data. <https://www.dwd.de/EN/ourservices/opendata/opendata.html>

Estonian Environment Agency Weather Services - ILM (n.d.). Observation data - Open Data <https://www.ilmateenistus.ee/>

European Commission and Directorate-General for Energy (2019). Study on Baltic offshore wind energy cooperation under BEMIP : final report. Publications Office.

Finnish Meteorological Institute - FMI (n.d.). Observation data - Open Data. <https://en.ilmatieteenlaitos.fi/open-data>.

Gravesen, H. and Kärnä, T. (2009). Ice loads for offshore wind turbines in Southern Baltic Sea. *In Proceedings of the International Conference on Port and Ocean Engineering Under Arctic Conditions*, number POAC9-3.

Heinonen, J. (2004). Constitutive modelling of ice rubble in first-year ridge keel. Master's thesis, Helsinki University of Technology.

Hendrikse, H. (2017). Ice-induced vibrations of vertically sided offshore structures.

Hendrikse, H., Owen, C. C. (2023). Application of the suggested ice strength coefficients in ISO 19906 to intermittent crushing. *In Proceedings of the 27th International Conference on Port and Ocean Engineering under Arctic Conditions*.

Hendrikse, H. and Nord, T. S. (2019). Dynamic response of an offshore structure interacting with an ice floe failing in crushing. *Marine Structures*, 65:271–290.

Hornnes, V., Hammer, T., Høyland, K. V., Hendrikse, H., and Turner, J. (2022). On the use of drift ice thickness statistics from a copernicus reanalysis product for fatigue damage calculation. *In Proceedings of the 26th IAHR International Symposium on Ice*.

Hornnes, V., Høyland, K. V., Turner, J. D., Gedikli, E. D., and Bjerkås, M. (2020). Combined distribution of ice thickness and speed based on local measurements at the Norströmsgrund lighthouse 2000-2003. *In proceedings of the 25<sup>th</sup> international symposium on ice Trondheim, Norway, 23rd–25th November 2020*. The International Association for Hydro-Environment Engineering and Research.

IEC (2019). Wind energy generation systems – part 3-1: Design requirements for fixed offshore wind turbines. *IEC 61400-3-1*.

Instytut Meteorologii i Gospodarki Wodnej Państwowy Instytut Badawczy - IMGW (n.d.). IMGW – Observation data - Open Data [https://danepubliczne.imgw.pl/data/dane\\_pomiarowo\\_obserwacyjne/dane\\_meteorologiczne/](https://danepubliczne.imgw.pl/data/dane_pomiarowo_obserwacyjne/dane_meteorologiczne/)

ISO19906, I. (2018). Petroleum and natural gas industries—arctic offshore structures. *Geneva: ISO*.

Jevrejeva, S., Drabkin, V., Kostjukov, J., Lebedev, A., Leppäranta, M., Mironov, Y. U., Schmelzer, N., and Sztobryn, M. (2004). Baltic sea ice seasons in the twentieth century. *Climate research*, 25(3):217–227.

Kärnä, T., Qu, Y., & Yue, Q. (2006). An extreme value analysis of local ice pressures. In *SNAME 7th International Conference and Exhibition on Performance of Ships and Structures in Ice*. OnePetro.

Latvian Environmental, Geology and Meteorology Centre - LVGMC (n.d.). Data upon request. <https://videscentrs.lvgtmc.lv/>

Leppäranta, M. and Omstedt, A. (1990). Dynamic coupling of sea ice and water for an ice field with free boundaries. *Tellus A: Dynamic Meteorology and Oceanography*, 42(4):482–495.

Nielsen, M. B., Hindhede, D., Palmer, M., and Thilsted, C. L. (2022). A highly efficient and rapid cost-optimization framework for offshore wind turbine foundations for an entire windfarm site. In *Proceedings of ASME 2022 International Offshore Wind Technical Conference (IOWTC2022)*, Boston, Massachusetts.

Rinker, J., Gaertner, E., Zahle, F., Skrzypinski, W., Abbas, N., Bredmose, H., ... & Dykes, K. (2020). Comparison of loads from HAWC2 and OpenFAST for the IEA Wind 15 MW Reference Wind Turbine. In *Journal of Physics: Conference Series* (Vol. 1618, No. 5, p. 052052). IOP Publishing.

Ronkainen, I., Lehtiranta, J., Lensu, M., Rinne, E., Haapala, J., and Haas, C. (2018). Interannual sea ice thickness variability in the bay of bothnia. *The Cryosphere*, 12(11):3459–3476.

Sveriges Meteorologiska och Hydrologiska Institut (n.d.) SMHI - Observationer Sverige. <https://www.smhi.se/en/weather/observations>.

Stap, F. van der. (2022). Ice-structure interaction in the Baltic Sea: defining a feasibility map for monopiles. Master's thesis, Delft University of Technology.

Stefan, J. (1891). Über die theorie der eisbildung, insbesondere über die eisbildung im polarmeere. *Annalen der Physik*, 278(2):269–286.

Tang, Y., Shi, W., You, J., and Michailides, C. (2021). Effects of nonlinear wave loads on large monopile offshore wind turbines with and without ice-breaking cone configuration. *Journal of Marine Science and Technology*, 26(1):37–53.

Thijssen, J., Fuglem, M., and Ralph, F. (2019). Level ice crushing pressures for estimating mooring loads. In *Proceedings of the 25th International Conference on Port and Ocean Engineering under Arctic Conditions (POAC)*, pages 9–13.

Timco, G. W., & Frederking, R. M. W. (1983). Flexural strength and fracture toughness of sea ice. *Cold Regions Science and Technology*, 8(1), 35-41.

WindEurope (2020). Offshore Wind in Europe Key trends and statistics 2020.

Wu, X., Hu, Y., Li, Y., Yang, J., Duan, L., Wang, T., Adcock, T., Jiang, Z., Gao, Z., Lin, Z., et al. (2019). Foundations of offshore wind turbines: A review. *Renewable and Sustainable Energy Reviews*, 104:379–393.

Zhu, B., Sun, C., and Jahangiri, V. (2021). Characterizing and mitigating ice-induced vibration of monopile offshore wind turbines. *Ocean Engineering*, 219:108406.